



**UCL**

**Palaeolimnological assessment of trace element inputs to lakes in the  
Athabasca Oil Sands Region, Alberta, Canada.**

**Interim report**

**ECRC Research Report Number 149**

**Neil L. Rose, Simon D. Turner & Handong Yang**

**March 2012**

## Contents

i)	Background and Aims	2
ii)	Scheme of work	2
iii)	Methods	5
iv)	Progress and data summary	6
	▪ Lithostratigraphic data	
	▪ Radiometric chronologies	
	▪ Trace element analysis	
	▪ Mercury analysis	
v)	Work outstanding	24
vi)	References	24

## **Background and Aims**

Undisturbed lake sediment records provide a robust natural archive of conditions within waterbodies. They have been used successfully over a number of decades to determine temporal trends of surface water acidification and to follow the effects of eutrophication. However, lake sediments also provide an archive of changes occurring within lake catchments and of atmospheric pollutants deposited onto lake and catchment surfaces. In August 2006, parallel lake sediment cores were collected from 22 lakes in the Athabasca Oil Sands Region of Alberta by UCL staff as part of the RAMP regional lakes survey. Twelve of these lakes were selected for study covering a range of locations from around the Fort McMurray area to sites in the Caribou Mountains and the Canadian Shield. The main aim of this initial study was to assess the evidence for lake acidification in the region, but analysis also revealed changes in nutrient input and, at one site, mercury (Hg) analysis showed an indication of industrial contamination. This work was reported in Curtis et al. (2010).

The analysis undertaken in this initial project was focussed on single radiometrically dated sediment cores (hereafter the 'A' cores) from each of the 12 selected lakes. The parallel cores from each lake (the 'B' cores) were stored dark, at 4°C, following their transfer to UCL and hence were available for further analysis. Both sediment cores (A and B) from the remaining 10 lakes remain unstudied.

The aim of this current project was to use the stored 'B' sediment cores to assess temporal trends and rates of change in trace element input to a subset of the lakes cored in the Athabasca Oil Sands Region of Alberta and compare these with the sediment records of two reference lakes in the Caribou Mountains.

This interim report contains details of progress on this work up to end March 2012 and a summary of remaining work under this contract. As a consequence this report focusses on data collected so far. Only limited interpretation is provided and will be undertaken fully when the dataset is complete. A final report will be produced upon completion of the study.

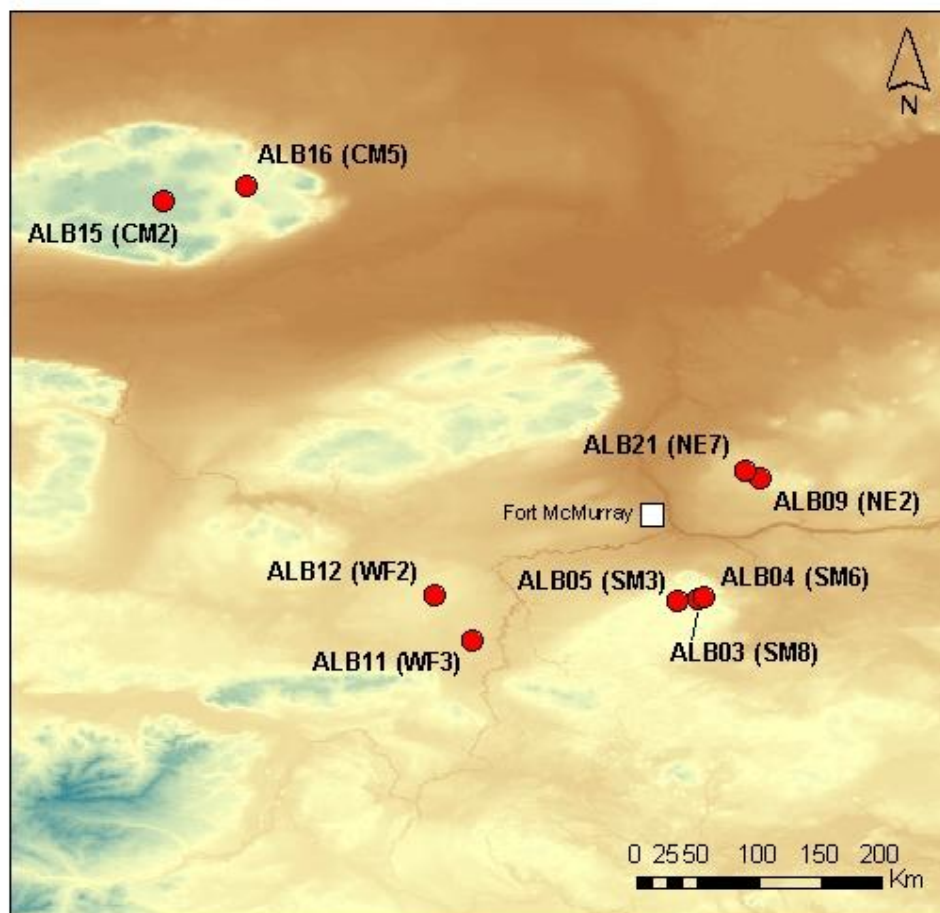
## **Scheme of work**

As a result of the work undertaken in the initial project, it is known that the sediment records from these lakes are robust and conformable and we have a reasonable estimate of the rate of sediment accumulation. However, the extent of the analyses undertaken on the 'A' cores resulted in there being very little material left upon which further work could be undertaken, especially in the upper levels and hence the current study uses the stored 'B' cores throughout. The advantage of using these 'B' cores is that we can be reasonably confident that the records should also be robust and conformable and we had a good idea what the accumulation rate was so analyses could be targeted prior to obtaining the final chronological data. The disadvantage is that, in order to produce reliable chronologies upon which to base any results (conversion of metal concentrations to fluxes; calculation of rates of change etc.) these 'B' cores also had to be radiometrically dated. Previous studies have used lithostratigraphic data from cores to cross-correlate dates from one to another, but the profiles from the 'A' cores have insufficient unambiguous 'tie-points' with which to do this and hence any dates ascribed in this manner to the 'B' cores would be rather inaccurate.

The scheme of work in the current study therefore uses the 'B' cores from nine of the original 12 selected lakes. These include NE2, NE7, WF2, WF3, SM3, SM6, SM8 in the Fort McMurray region plus two lakes from the Caribou Mountains, CM2 and CM5, which may be considered

'reference lakes'. The locations of these sites are shown in Figure 1. These lakes and cores are also known by different codes. Table 1 is a translation Table to ensure clarity in this matter.

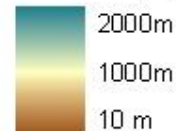
**Figure 1. Location map of lakes used in the current study**



Lake Sites used in this report  
CEMA codes in brackets

Background map GLOBE (NOAA) DEM  
Spatial reference: WGS 1984

**Altitude (m)**



The work falls under five tasks:

1. Lithostratigraphic analysis.

This work provides the basic information required for sediment dating, compositional changes and interpretation of trace element inputs. Sediment samples from each level were analysed for water content, organic matter content (by loss-on-ignition at 550°C) carbonate content (loss-on-ignition at 950°C) and sediment bulk wet density measurements at regular intervals down the core.

## 2. Radiometric chronologies

A reliable chronology is the basis of all palaeolimnological investigation and allows dates and rates of change to be determined. Lead-210 (half-life 22.3 year) is a naturally-produced radionuclide, derived from atmospheric fallout (termed unsupported  $^{210}\text{Pb}$ ). Cesium-137 (half-life 30 years) and  $^{241}\text{Am}$  are artificially produced radionuclides, introduced to the study area by atmospheric fallout from nuclear weapons testing and nuclear reactor accidents. They have been extensively used in the dating of recent sediments. Sediment samples from each core were analysed for  $^{210}\text{Pb}$ ,  $^{226}\text{Ra}$ ,  $^{137}\text{Cs}$  and  $^{241}\text{Am}$  by direct gamma assay. Core chronologies were calculated from these data using a choice or combination of two models, the CRS (constant rate of supply) or CIC (constant initial concentration) models.

## 3. Element analysis

Sediment samples from each core were analysed for a requested suite of elements: Al, As, Ba, Cr, Cu, Fe, Mn, Ni, Pb, Se, Sr, Ti and Zn. This list is compiled from elements linked to deposition in the Athabasca region adjacent to mining activity as well as those possibly associated with aeolian transport of mine dust (Rod Hazewinkel e-mail 16<sup>th</sup> May 2011). It also includes a number of the priority pollutant elements (PPEs) of concern due to concentrations in deposition and waters in the Athabasca River area (Kelly et al 2010).

## 4. Mercury analysis.

Mercury (Hg) is a very important element in contamination studies and elevated levels have already been recorded in the upper levels of sediments in this region (Curtis et al. 2010). Mercury was analysed in each core at the same resolution as for the other trace elements.

## 5. Reporting and manuscript preparation

In addition to a final report, we will prepare a manuscript on the results of this work that will be submitted to an international peer-reviewed journal.

**Table 1. Core code ‘translation’ table for sites used in this study**

Core ID	Alternative site name	Alternative site code	Coring date	Latitude	Longitude	Coring depth (m)	Core length (cm)
ALB03B	287	SM8	22 Aug 2006	56.216	111.205	1.4	18.5
ALB04B	A26	SM6	22 Aug 2006	56.222	111.170	1.6	23
ALB05B	289	SM3	22 Aug 2006	56.202	111.364	3.1	25.5
ALB09B	L7	NE2	23 Aug 2006	57.093	110.750	1.65	28.5
ALB11B	A59	WF3	24 Aug 2006	55.909	112.865	1.2	23.5
ALB12B	A47	WF2	24 Aug 2006	56.246	113.141	1.6	42
ALB15B	E59 (Rocky Island)	CM2	25 Aug 2006	59.119	115.128	5.5	34.5
ALB16B	O1 (Unnamed #6)(E55)	CM5	25 Aug 2006	59.238	114.524	1.3	24
ALB21B	185	NE7	30 Aug 2006	57.147	110.865	1.5	24

## Methods

### Lithostratigraphy

Sediment water content was determined gravimetrically by determining sample weight-loss after heating at 105°C for 24 hours. Organic matter content and carbonate content were similarly determined by measuring weight-loss after heating to 550°C for 2 hours and 950°C for 2 hours respectively (Heiri *et al* 2001). Wet density measurements were undertaken on every sixth sample by evenly filling wet sediment into a 2 cm<sup>3</sup> measurement vial and weighing on an electronic analytical balance to four decimal places.

### Radiometric core chronologies

Dried sediment samples were analysed for <sup>210</sup>Pb, <sup>226</sup>Ra, <sup>137</sup>Cs and <sup>241</sup>Am by direct gamma assay in the University College London Department of Geography Gamma Spectroscopy Laboratory, using ORTEC HPGe GWL series well-type coaxial low background intrinsic germanium detectors. Lead-210 was determined via its gamma emissions at 46.5keV, and <sup>226</sup>Ra by the 295keV and 352keV gamma rays emitted by its daughter isotope <sup>214</sup>Pb following three weeks storage in sealed containers to allow radioactive equilibration. Cesium-137 and <sup>241</sup>Am were measured by their emissions at 662keV and 59.5keV (Appleby *et al*, 1986). The absolute efficiencies of the detector were determined using calibrated sources and sediment samples of known activity. Corrections were made for the effect of self absorption of low energy gamma rays within the sample (Appleby *et al*, 1992).

### Elemental analysis

Sediment samples were analysed for trace elements using a Spectro XLAB2000 X-ray fluorescence (XRF) spectrometer. This enables automated elemental analysis of major, minor and trace elements from sodium (Na) to uranium (U) and allows both rapid exploratory analysis as well as the possibility of more detailed, low detection analytical work for targeted elements. We analysed c.30 samples in each core depending on the length of the post-1850 sediment record to provide a high resolution temporal record of each element in each lake. Analysis included a selection of samples from 'pre-industrial' sediment depths within each core to get 'background' values for each site. 1g of freeze dried sediment was placed in nylon cups with a base of prolene foil (4 µm thickness). Freeze dried sediments were crushed to a fine powder in their original sample bags. After pouring into the containers, the powder was slightly pressed with a pestle. Due to the low sample mass and very organic nature of the sediments, this was essential to maintain the sediment sample within the cups. Two reference sediment (Buffalo River Sediment NIST- RM8704) samples (precisely weighed samples of c. 1g and 2g) were included in each sample batch run to identify any machine drift error and assess measurement accuracy. Means, standard deviations and percentage recoveries for these are shown in Table 2. Recovery varies by element but ranges between 90.5% (Ba) and 109.9% (Al). For pollutant elements of particular interest, recovery is 97.9%, 97.0%, 91.0% and 102.7% for Ni, Zn, As and Pb respectively. Additional certified reference materials will be used for those elements not covered by the Buffalo River certification.

### Mercury analysis

Sediment samples for Hg analysis were freeze-dried. Samples were digested with 8 ml aqua regia at 100 °C on a hotplate for 2 hours in rigorously acid-leached 50 ml Teflon beakers. Standard reference material (stream sediment GBW07305) and sample blanks were digested with each batch of 20 samples. Digested solutions were analysed for Hg using cold vapour-atomic fluorescence spectrometry (CV-AFS) following reduction with SnCl<sub>2</sub>. Standard solutions and quality control blanks were measured every five samples to monitor measurement stability.

**Table 2. Measured and reported values for element concentrations in Buffalo River sediment (NIST8704) for two different sediment sample weights.**

	Al	Ti	Cr	Mn	Fe	Ni	Cu	Zn	As	Se	Sr	Ba	Pb
	%	%	%	%	%	µg/g	µg/g	µg/g	µg/g	µg/g	µg/g	µg/g	µg/g
Mean (1g)	6.706	0.491	0.01265	0.0542	4.308	42.000	89.850	395.675	15.475	0.975	128.175	373.650	154.100
SD (1g)	0.091	0.007	0.00036	0.00013	0.0372	0.458	3.702	2.919	0.228	0.238	2.351	17.926	1.742
% Recovery (1g)	109.94	107.37	103.75	99.59	108.51	97.90		96.98	91.03			90.47	102.73
Mean (2g)	6.518	0.479	0.013	0.054	4.276	41.250	87.300	398.650	14.800	1.050	126.500	342.025	150.250
SD (2g)	0.130	0.005	0.001	0.001	0.018	0.934	3.749	4.922	1.017	0.229	1.102	5.590	2.644
Recovery (2g)	106.85	104.85	105.74	99.45	107.70	96.15		97.71	87.06			82.81	100.17
NIST RM8704 Values	6.1	0.457	0.01219	0.0544	3.97	42.9 ...		408	17	...	...	413	150

Note: NIST values (...) not known; As (17) for information only. We will also run CANMET-LKSD2 reference sediment in runs with samples to capture Cu and Sr

## Progress and Data Summary

### Lithostratigraphic data

Lithostratigraphic analysis provides essential background data for the chronological work and interpretation of the trace element data. All this work has been completed. Percentage dry weight, percentage organic matter (as measured by LOI 550°C) and percentage carbonate content (as measured by LOI 950°C) for all nine 'B' cores are presented in Figures 2, 3 and 4 respectively. In addition, Figure 3 shows the LOI 550°C data for the nine 'B' cores plotted along with the 'A' cores analysed as part of the previous study (reported in Curtis et al., 2010). These data show a very good level of consistency between the 'A' and 'B' cores which allows great confidence in the comparison between the two datasets and subsequent interpretation.

Figure 2. Percentage dry weight data for the 9 'B' cores

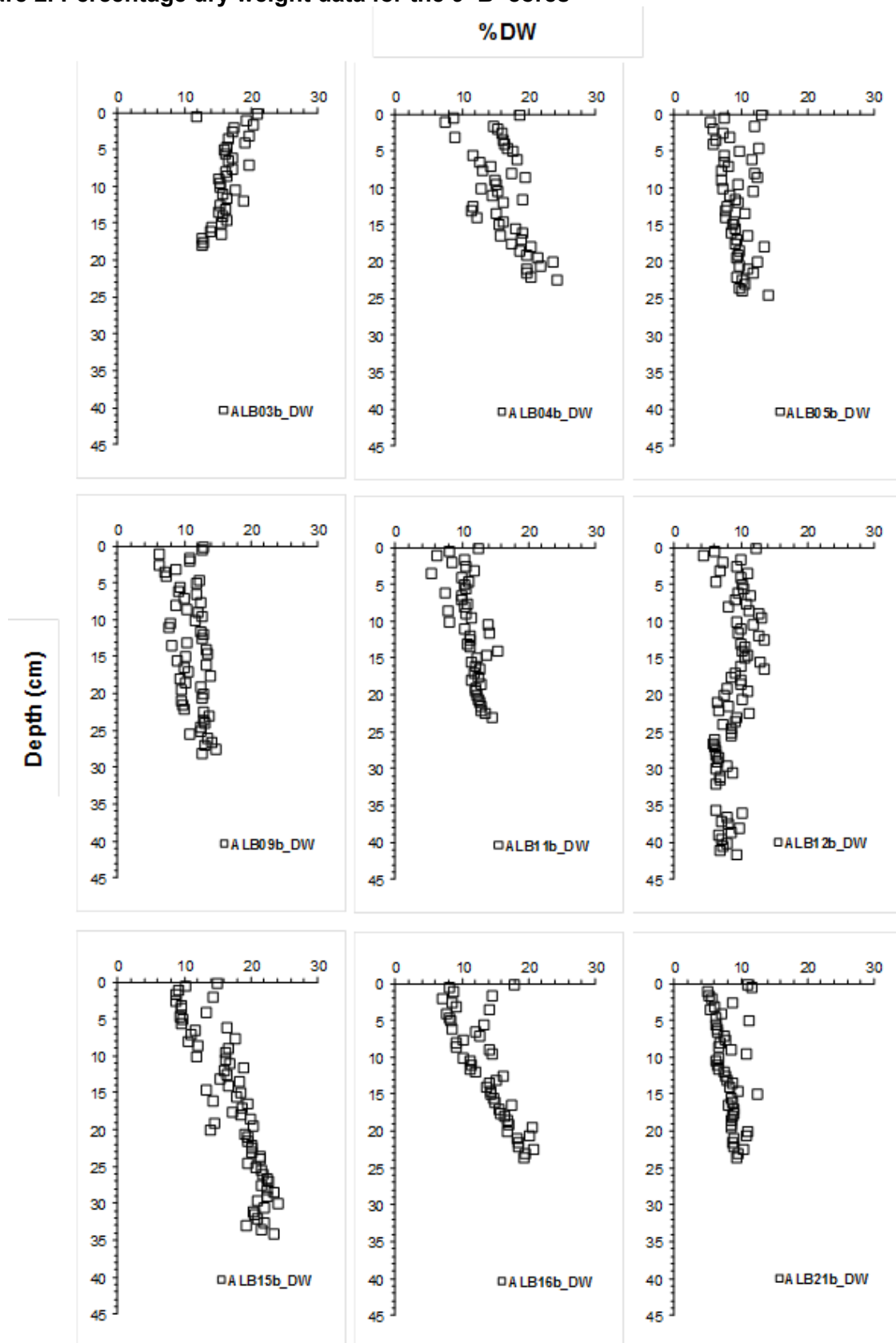




Figure 3. Percentage organic matter (LOI 550°C) for the 9 'B' cores (open circles) and comparison with the same data from the equivalent 'A' cores (shaded squares).

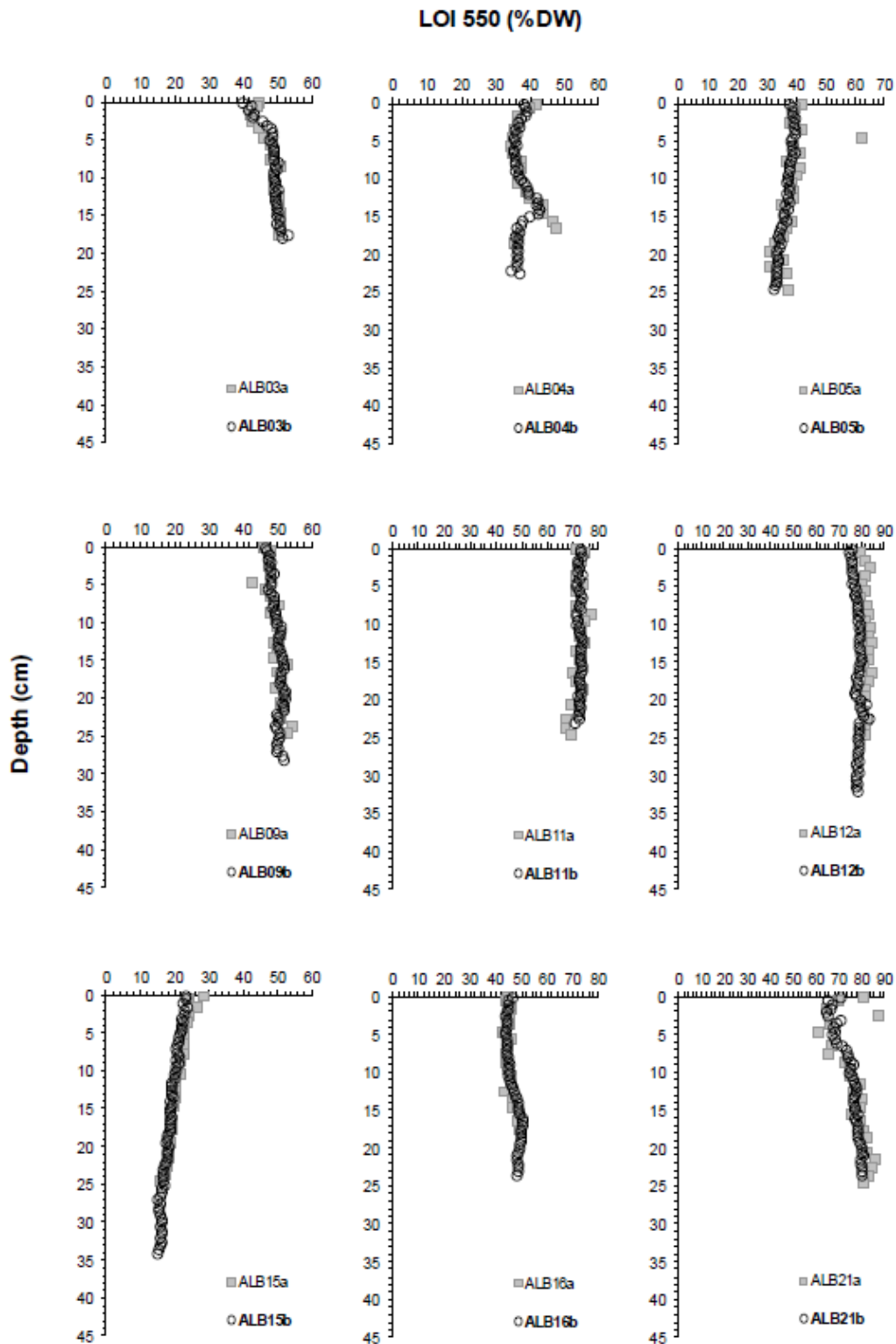
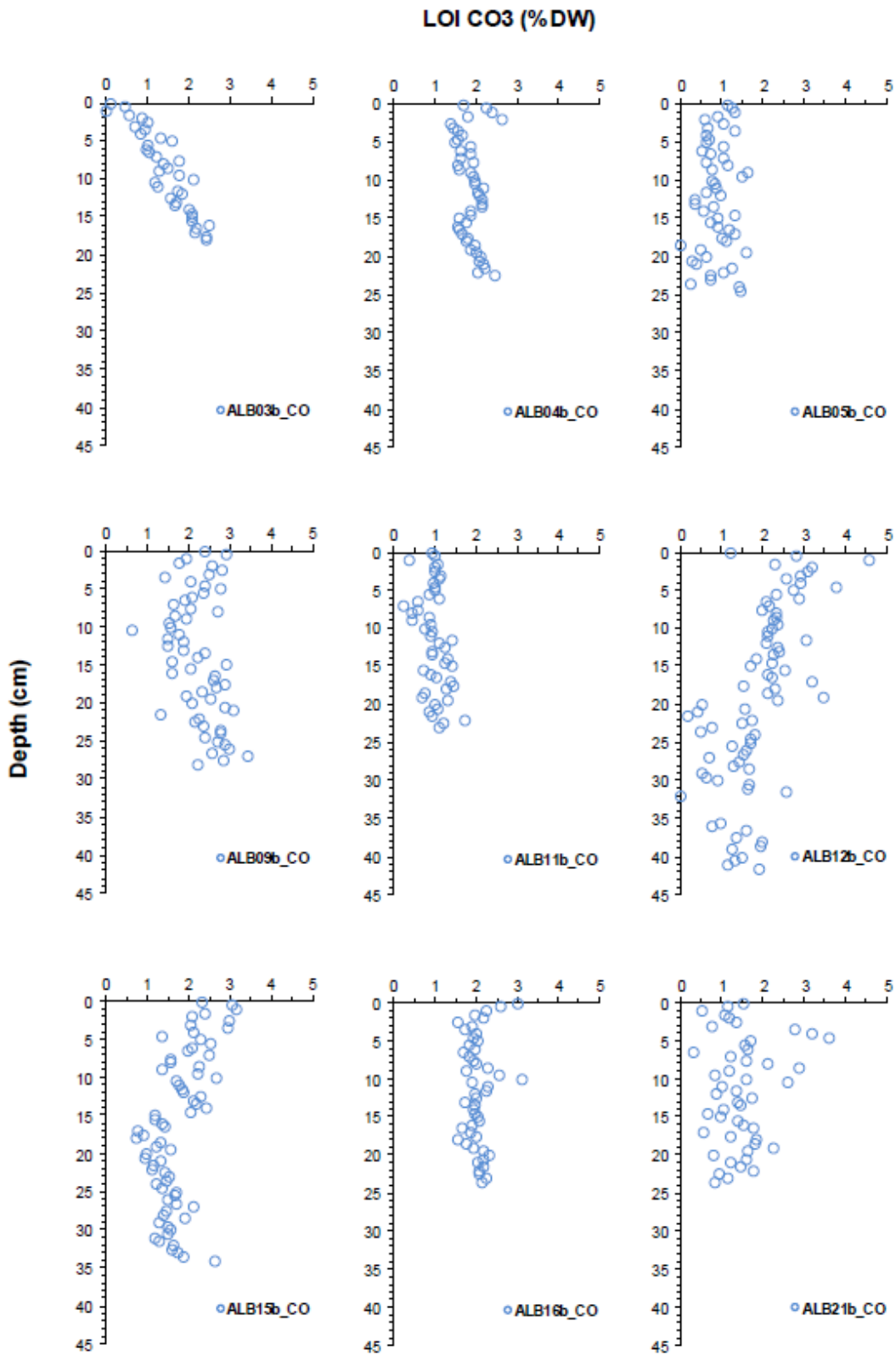


Figure 4. Percentage carbonate content (LOI 950°C) for the 9 'B' cores



### Chronological data

Radiometric measurements have been completed on ALB03B, ALB04B, ALB05B and ALB11B. Here, we summarise these data and the derived sediment chronologies for these cores.

#### **i) ALB03B**

##### *Lead-210 Activity*

Equilibrium of total  $^{210}\text{Pb}$  activity with supporting  $^{210}\text{Pb}$ , seems to occur at a sediment depth of c. 7 cm. Unsupported  $^{210}\text{Pb}$  activities, calculated by subtracting supporting  $^{210}\text{Pb}$  activity from total  $^{210}\text{Pb}$  activity (Table 3; Fig 5a), decline irregularly with depth (Figure 5b). Departures from a  $^{210}\text{Pb}$  exponential decline in the top 3 cm are smaller than those below, suggesting changes in sedimentation rates are reduced in this section of the core.

##### *Artificial Fallout Radionuclides*

The  $^{137}\text{Cs}$  activity versus depth profile (Table 4; Figure 5c) has well-resolved peaks. Peaks around 0.75 and 2.25 cm are likely to be derived from the 1986 Chernobyl accident fallout and the 1963 fallout maximum from the atmospheric testing of nuclear weapons, respectively.

##### *Core Chronology*

Use of the CIC model was precluded by the non-monotonic features in the unsupported  $^{210}\text{Pb}$  profile.  $^{210}\text{Pb}$  dates were calculated using the CRS model (Appleby 2001) which places 1963 and 1986 at c. 2 and 1 cm, respectively. These are in agreement with the  $^{137}\text{Cs}$  record. The CRS model chronologies and sediment accumulations calculated using  $^{210}\text{Pb}$  data in the core are shown in Table 5 and Figure 6. This indicates that there were some changes in sediment accumulation around the beginning of the 20<sup>th</sup> century followed by relatively uniform sedimentation rates with a mean of c.  $0.0071 \text{ g cm}^{-2} \text{ yr}^{-1}$  since the 1920s.

**Table 3.  $^{210}\text{Pb}$  concentrations in core ALB03B.**

Depth cm	Dry Mass $\text{g cm}^{-2}$	Total		Pb-210 Supported		Unsupp		Cum Unsupported Pb-210	
		$\text{Bq Kg}^{-1}$	$\pm$	$\text{Bq Kg}^{-1}$	$\pm$	$\text{Bq Kg}^{-1}$	$\pm$	$\text{Bq m}^{-2}$	$\pm$
0.25	0.0175	245.18	28.57	30.89	6.59	214.29	29.32	39.2	4.1
0.75	0.07	211.59	17.85	32.87	4.35	178.72	18.37	142.1	12.9
1.25	0.1609	182.63	18.38	31.51	4.46	151.12	18.91	291.8	21.1
1.75	0.2519	100.09	17.13	39.77	4.65	60.32	17.75	381.7	27.5
2.25	0.3564	85.06	11.3	39.77	3.24	45.29	11.76	436.5	32.2
2.75	0.461	72.09	13.42	35.64	4.05	36.45	14.02	479.1	34.8
3.25	0.5568	46.69	11.13	40.99	3.06	5.7	11.54	494.9	37.2
3.75	0.6526	73.59	14.89	29.92	3.82	43.67	15.37	512.8	39.1
4.25	0.7452	47.4	6.71	43.25	2.19	4.15	7.06	528.4	41.2
4.75	0.8378	48.5	8.97	43.66	2.84	4.84	9.41	532.5	41.8
5.25	0.9284	51.29	9.4	33.45	2.29	17.84	9.67	541.5	42.7
5.75	1.0189	44.02	7.84	42.73	2.64	1.29	8.27	547.2	43.5
6.75	1.2	37.6	9.7	36.75	2.7	0.85	10.07	549.2	45.7

**Table 4. Artificial fallout radionuclide concentrations in core ALB03B.**

Depth cm	Cs-137		Am-241	
	Bq kg <sup>-1</sup>	±	Bq kg <sup>-1</sup>	±
0.25	108.46	5.78	0	0
0.75	110.1	4.24	0	0
1.25	95.77	4.43	0	0
1.75	54.37	3.15	0	0
2.25	62.14	2.71	0	0
2.75	40.55	3	0	0
3.25	26.18	1.94	0	0
3.75	14.97	2.02	0	0
4.25	20.62	1.27	0	0
4.75	15.38	1.54	0	0
5.25	9.45	1.16	0	0
5.75	12.1	1.47	0	0
6.75	3.4	1.25	0	0

**Table 5. <sup>210</sup>Pb chronology of core ALB03B**

Depth cm	Drymass g cm <sup>-2</sup>	Chronology			Sedimentation Rate		
		Date AD	Age yr	±	g cm <sup>-2</sup> yr <sup>-1</sup>	cm yr <sup>-1</sup>	± %
0	0	2006	0				
0.25	0.0175	2004	2	2	0.0074	0.079	16.6
0.75	0.07	1996	10	2	0.0071	0.049	15.3
1.25	0.1609	1982	24	4	0.0053	0.029	20.7
1.75	0.2519	1968	38	6	0.0086	0.044	37.2
2.25	0.3564	1955	51	9	0.0077	0.037	41.3
2.75	0.461	1940	66	14	0.0059	0.029	61.3
3.25	0.5568	1928	78	18	0.0086	0.045	73.3
3.75	0.6526	1918	88	25	0.0025	0.013	86.3
4.25	0.7452	1912	94	29	0.0167	0.09	100.2
4.75	0.8378	1896	110	35	0.0057	0.031	112.8

Figure 5. Fallout radionuclide concentrations in core ALB03B showing (a) total  $^{210}\text{Pb}$ , (b) unsupported  $^{210}\text{Pb}$ , and (c)  $^{137}\text{Cs}$  concentrations versus depth.

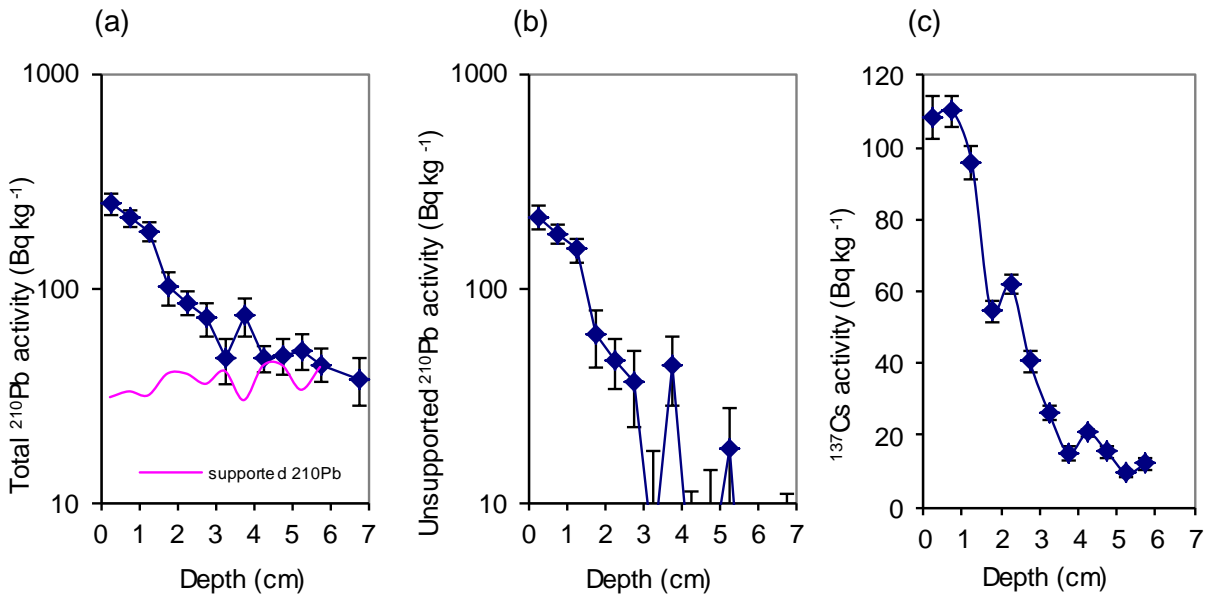
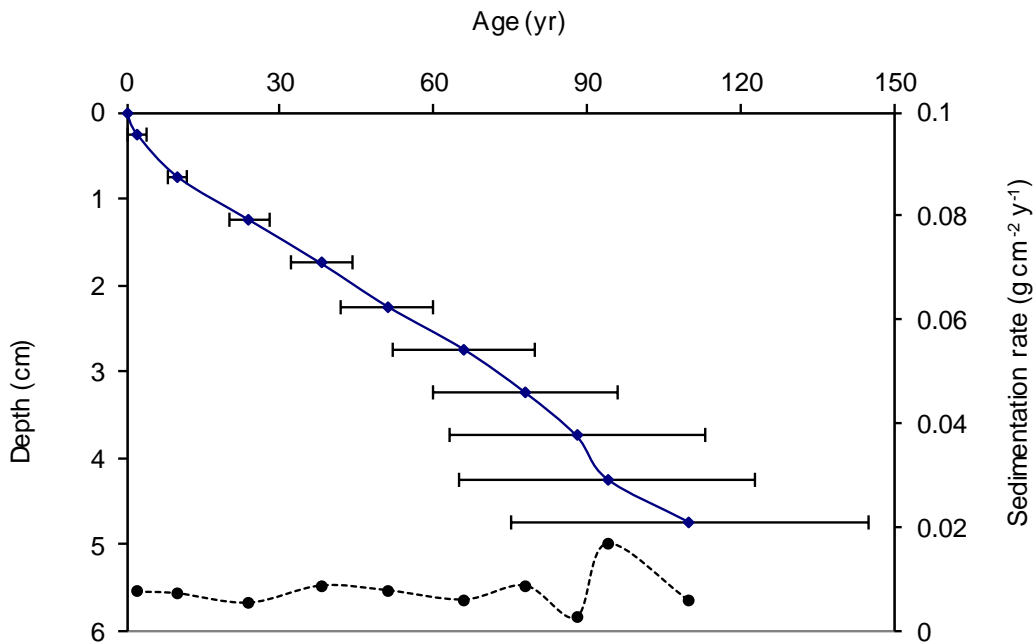


Figure 6. Radiometric chronology of core ALB03B showing the CRS model  $^{210}\text{Pb}$  dates and sedimentation rates. The solid line shows age while the dashed line indicates sedimentation rate.



## ii) ALB04B

### Lead-210 Activity

The equilibrium depth of total  $^{210}\text{Pb}$  activity (Table 6; Figure 7a) with the supporting  $^{210}\text{Pb}$  is at around 10 cm in this core. The maximum value of unsupported  $^{210}\text{Pb}$  is at 2.25 cm (Figure 7b), suggesting an increase in sediment accumulation rate in the recent years. Below the sediment surface,  $^{210}\text{Pb}$  activities decline irregularly but smoothly, implying that sedimentation rates have changed only gradually over this period.

### Artificial Fallout Radionuclides

The  $^{137}\text{Cs}$  activity versus depth profile (Figure 7c) shows a peak at 2.25 cm. However,  $^{241}\text{Am}$  was detected at around 4.25 cm (Table 7; Figure 7c). As  $^{241}\text{Am}$  was produced in atmospheric nuclear weapons tests but not in the Chernobyl accident, this would indicate that 1963 is at around 4.25 cm. The more recent peak of  $^{137}\text{Cs}$  at 2.25 cm is therefore likely to be derived from the 1986 Chernobyl accident fallout.

### Core Chronology

As with ALB03B, use of the CIC model was precluded in this core by the non-monotonic features in the unsupported  $^{210}\text{Pb}$  profile (Figure 7b). The CRS dating model places 1963 and 1986 at c. 4.5 and 2.5 cm, respectively, which are in good agreement with the  $^{137}\text{Cs}$  and  $^{241}\text{Am}$  records. The CRS model chronologies and sediment accumulation rates for this core are shown in Table 8 and Figure 8. Overall, there has been a gradual increase in sediment accumulation over the 20<sup>th</sup> century from c. 0.006 to 0.019 g cm<sup>-2</sup> yr<sup>-1</sup>. This was followed by a rapid increase to 0.052 g cm<sup>-2</sup> yr<sup>-1</sup> in the last few years (to 2006). There may have been some changes in sedimentation rates before 1900, but confidence limits on these data are large and need to be considered with any interpretation.

**Table 6.  $^{210}\text{Pb}$  concentrations in core ALB04B**

Depth cm	Dry Mass g cm <sup>-2</sup>	Total		Pb-210				Cum Unsupported Pb-210	
		Bq Kg <sup>-1</sup>	±	Supported Bq Kg <sup>-1</sup>	±	Unsupp Bq Kg <sup>-1</sup>	±	Bq m <sup>-2</sup>	±
0.25	0.021	187.11	23.66	53.42	7.06	133.69	24.69	27.6	3.9
1.25	0.1218	385.71	46.94	60.35	12.03	325.36	48.46	244.8	31.1
2.25	0.256	371.9	21.89	42.73	5.22	329.17	22.5	683.8	65.7
3.25	0.4132	342.95	30.61	40.9	6.7	302.05	31.33	1179.6	79.9
4.25	0.5794	265.53	28.93	44.97	7.03	220.56	29.77	1610.5	97.1
5.25	0.7417	179.26	21.92	43.41	5.41	135.85	22.58	1894.2	108.4
6.25	0.8972	125.45	18.21	38.54	4.39	86.91	18.73	2064.6	114
7.25	1.0642	86.53	15.35	42.42	4.4	44.11	15.97	2170	117.9
8.25	1.2427	56.26	9.01	45.98	2.98	10.28	9.49	2211.5	120.7
9.25	1.4297	52.12	11.1	40.09	2.95	12.03	11.49	2232.3	122.1
9.75	1.5274	41.25	11.75	34.84	3.07	6.41	12.14	2241	122.9

**Table 7. Artificial fallout radionuclide concentrations in core ALB04B.**

Depth cm	Cs-137		Am-241	
	Bq Kg <sup>-1</sup>	±	Bq Kg <sup>-1</sup>	±
0.25	79.56	5.4	0	0
1.25	193.9	12.4	0	0
2.25	201.13	6.11	0	0
3.25	172.34	7.12	0	0
4.25	126.75	5.99	5.82	2.74
5.25	74.28	4.28	0	0
6.25	47.45	3.14	0	0
7.25	25.62	2.34	0	0
8.25	17.98	1.6	0	0
9.25	12.87	1.54	0	0
9.75	10.97	1.67	0	0

**Table 8. <sup>210</sup>Pb chronology of core ALB04B**

Depth cm	Drymass g cm <sup>-2</sup>	Chronology			Sedimentation Rate		
		Date AD	Age yr	±	g cm <sup>-2</sup> yr <sup>-1</sup>	cm yr <sup>-1</sup>	± %
0	0	2006	0				
0.25	0.021	2006	0	2	0.0519	0.532	18.4
1.25	0.1218	2002	4	2	0.0192	0.164	15.8
2.25	0.256	1994	12	2	0.0149	0.102	9.3
3.25	0.4132	1982	24	2	0.0111	0.069	12.9
4.25	0.5794	1966	40	3	0.0091	0.055	16.8
5.25	0.7417	1947	59	5	0.0083	0.052	21.7
6.25	0.8972	1927	79	7	0.0068	0.042	30
7.25	1.0642	1901	105	11	0.006	0.034	48.9
8.25	1.2427	1879	127	16	0.013	0.071	102.3
9.25	1.4297	1857	149	16	0.0057	0.03	104.5

Figure 7. Fallout radionuclide concentrations in core ALB04B showing (a) total  $^{210}\text{Pb}$ , (b) unsupported  $^{210}\text{Pb}$ , and (c)  $^{137}\text{Cs}$  and  $^{241}\text{Am}$  concentrations versus depth.

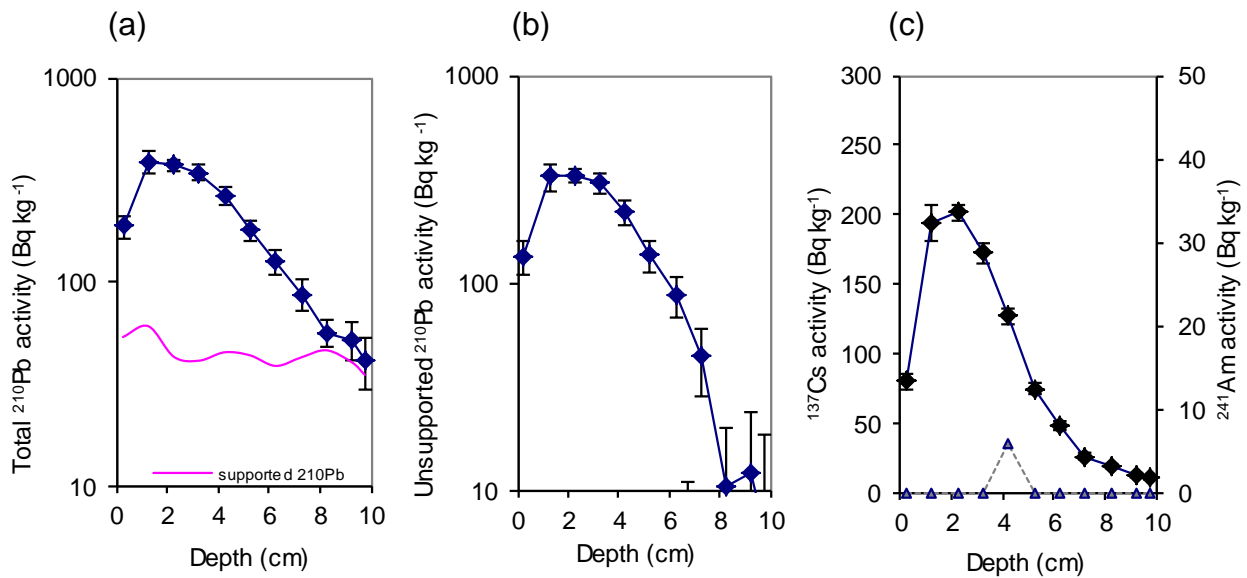
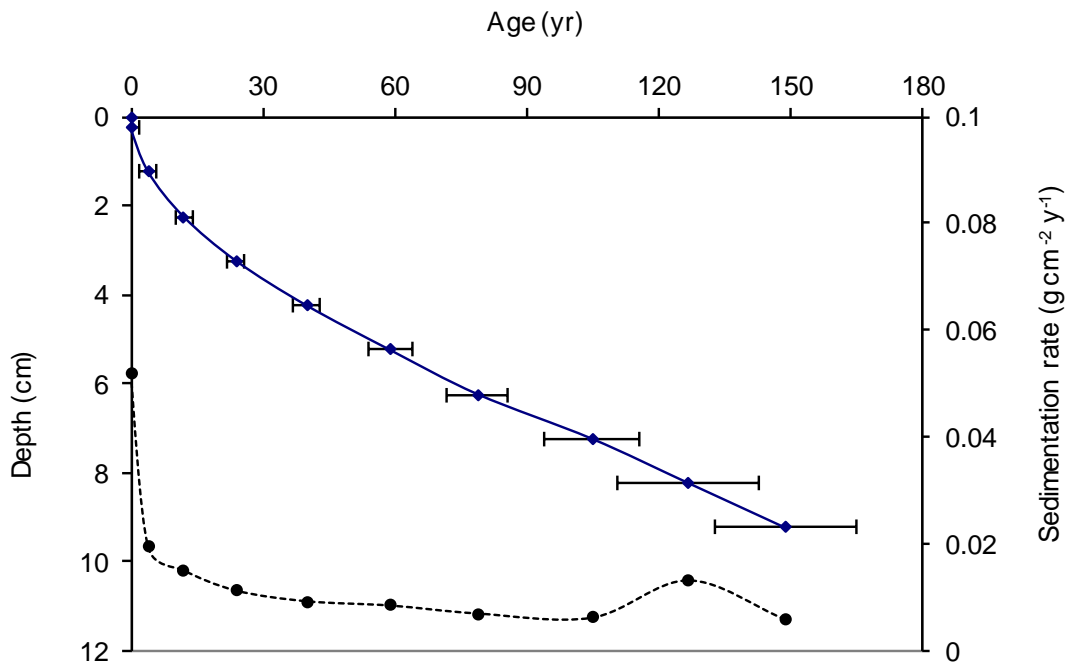


Figure 8. Radiometric chronology of core ALB04B showing the CRS model  $^{210}\text{Pb}$  dates and sedimentation rates. The solid line shows age while the dashed line indicates sedimentation rate.





### iii) ALB05B

#### Lead-210 Activity

This core does not reach the equilibrium depth of total  $^{210}\text{Pb}$  activity with the supporting  $^{210}\text{Pb}$  at the base (Table 9; Figure 9a). The unsupported  $^{210}\text{Pb}$  profile can be divided into two sections (Figure 9b). From 0 to 11.5 cm, there is little net decline in unsupported  $^{210}\text{Pb}$  activities, suggesting an increase in sediment accumulation in the recent years. From 12 cm to the base of the core, overall unsupported  $^{210}\text{Pb}$  activities decline more or less exponentially with depth, but with some small changes, suggesting that sedimentation rates were relatively stable.

#### Artificial Fallout Radionuclides

The  $^{137}\text{Cs}$  activity versus depth profile (Figure 9c) shows two relatively broad peaks at around 6.25 and 14.25 cm that almost certainly record the 1986 Chernobyl accident fallout and the 1963 fallout maximum from the atmospheric testing of nuclear weapons, respectively.

#### Core Chronology

Non-monotonic features in the unsupported  $^{210}\text{Pb}$  profile precluded the use of the CIC model. The simple CRS dating model puts 1963 and 1986 depths at c. 13 and 8.3 cm, respectively, which are reasonable in agreement with the  $^{137}\text{Cs}$  record. The  $^{210}\text{Pb}$  sediment accumulation rate indicates that sedimentation rates were relatively uniform with a slight increase from the 1870s to the 1970s and a mean of  $0.015 \text{ g cm}^{-2} \text{ yr}^{-1}$ . In the last 30 years or so, sedimentation rates have significantly increased to c.  $0.05 \text{ g cm}^{-2} \text{ yr}^{-1}$  (Figure 10; Table 11).

**Table 9.  $^{210}\text{Pb}$  concentrations in core ALB05B taken from an Albertan lake, Canada.**

Depth cm	Dry Mass $\text{g cm}^{-2}$	Total		Pb-210 Supported		Unsupp		Cum Unsupported Pb-210	
		$\text{Bq kg}^{-1}$	$\pm$	$\text{Bq kg}^{-1}$	$\pm$	$\text{Bq kg}^{-1}$	$\pm$	$\text{Bq m}^{-2}$	$\pm$
0.5	0.041	334.79	20.37	34.09	4.28	300.7	20.81	124.1	8.7
3.25	0.3056	326.91	32.55	36.78	7.67	290.13	33.44	905.7	67.5
6.25	0.5907	327.83	20.7	38.38	4.62	289.45	21.21	1731.8	116.9
8.25	0.7576	269.76	21.99	46.21	5.71	223.55	22.72	2157.5	125.9
10.25	0.9828	383.83	37.2	52.3	9.17	331.53	38.31	2774.7	142.6
12.25	1.1967	309.43	22.94	40.85	5.08	268.58	23.5	3414.2	164.9
14.25	1.3753	237.8	14.81	44.95	3.73	192.85	15.27	3822.6	171.2
16.25	1.5796	141.03	13.11	41.92	3.53	99.11	13.58	4110.2	174.3
17.25	1.6887	137.98	15.72	29.72	3.49	108.26	16.1	4223.2	175.4
20.25	2.0135	111.07	15.07	34.91	3.68	76.16	15.51	4519.7	181
22.25	2.2262	106.09	15.7	31.39	3.75	74.7	16.14	4680.1	185
23.25	2.3456	72.46	9.24	43.92	2.93	28.54	9.69	4737.4	186.3
24.75	2.5436	62.02	7.31	41.34	2.07	20.68	7.6	4785.7	187

**Table 10. Artificial fallout radionuclide concentrations in core ALB05B.**

Depth cm	Cs-137		Am-241	
	Bq kg <sup>-1</sup>	±	Bq kg <sup>-1</sup>	±
0.5	137.09	4.53	0	0
3.25	153.47	8.5	0	0
6.25	170.83	5.55	0	0
8.25	162.92	6.26	0	0
10.25	133.15	7.76	0	0
12.25	138.81	5.34	0	0
14.25	151.32	4.19	0	0
16.25	116.41	3.65	0	0
17.25	68.78	3.12	0	0
20.25	26.8	2.42	0	0
22.25	22.7	2.25	0	0
23.25	16.73	1.66	0	0
24.75	8.04	1.07	0	0

**Table 11. <sup>210</sup>Pb chronology of core ALB05B taken from an Albertan lake, Canada.**

Depth cm	Drymass g cm <sup>-2</sup>	Chronology			Sedimentation Rate		
		Date AD	Age yr	±	g cm <sup>-2</sup> yr <sup>-1</sup>	cm yr <sup>-1</sup>	± %
0	0	2006	0				
0.5	0.041	2005	1	2	0.0491	0.522	8
3.25	0.3056	1999	7	2	0.0425	0.445	12.2
6.25	0.5907	1992	14	2	0.0337	0.373	8.7
8.25	0.7576	1987	19	2	0.0377	0.385	11.3
10.25	0.9828	1979	27	2	0.0197	0.179	12.6
12.25	1.1967	1967	39	2	0.0169	0.172	10.7
14.25	1.3753	1957	49	3	0.0169	0.176	11.1
16.25	1.5796	1946	60	4	0.0238	0.228	17
17.25	1.6887	1941	65	4	0.0185	0.171	18.4
20.25	2.0135	1921	85	5	0.0142	0.132	25.4
22.25	2.2262	1901	105	8	0.0078	0.071	32.2
23.25	2.3456	1890	116	11	0.0142	0.112	46.7
24.75	2.5436	1875	131	16	0.0123	0.095	54.4

Figure 9. Fallout radionuclide concentrations in core ALB05B showing (a) total  $^{210}\text{Pb}$ , (b) unsupported  $^{210}\text{Pb}$ , and (c)  $^{137}\text{Cs}$  concentrations versus depth.

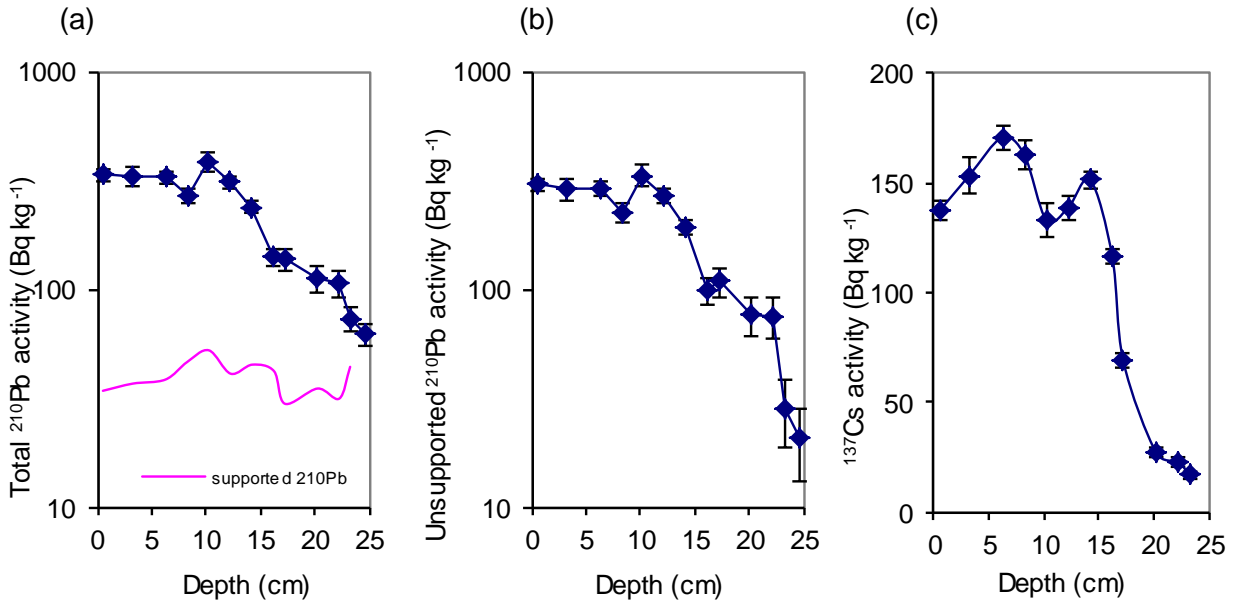
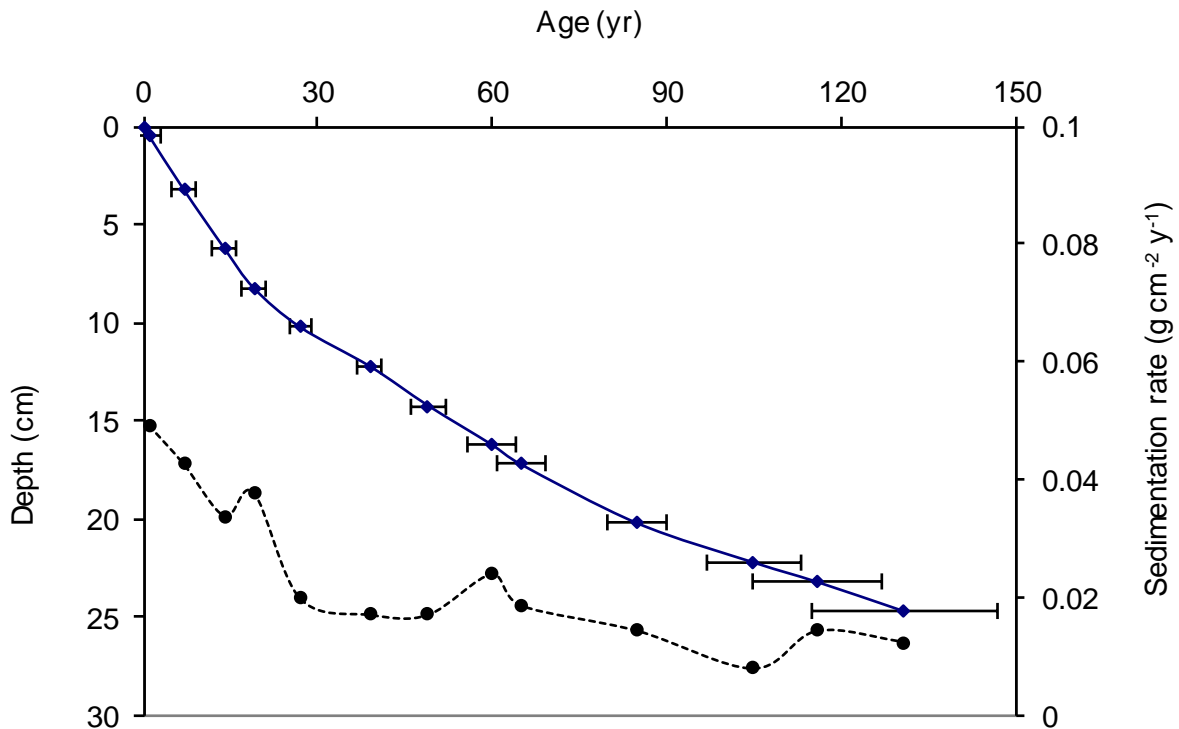


Figure 10. Radiometric chronology of core ALB05B showing the CRS model  $^{210}\text{Pb}$  dates and sedimentation rates. The solid line shows age while the dashed line indicates sedimentation rate.



#### iv) ALB11B

##### *Lead-210 Activity*

It seems that equilibrium depth of total  $^{210}\text{Pb}$  activity with the supporting  $^{210}\text{Pb}$  is at around 20.5 cm of this core (Table 12; Figure 11a). Similar to core ALB05B, there is little net decline in unsupported  $^{210}\text{Pb}$  activities in the upper 6.5 cm, and the maximum activity is at 6.25 cm (Figure 11b), suggesting an increase in sediment accumulation in the recent years. From 6.5 to 20.5 cm, unsupported  $^{210}\text{Pb}$  activities decline more or less exponentially with depth but with a dip at 14.25 cm, suggesting a relatively uniform sediment accumulation with an increased sedimentation rate at around 14.25 cm.

##### *Artificial Fallout Radionuclides*

The  $^{137}\text{Cs}$  activity versus depth profile (Figure 11c; Table 13) shows a well resolved peak at 8.25 cm. The presence of a poorly resolved  $^{241}\text{Am}$  peak at this depth confirms that this  $^{137}\text{Cs}$  peak records the 1963 fallout maximum from the atmospheric testing of nuclear weapons.

##### *Core Chronology*

Figure 12 (and Table 14) shows  $^{210}\text{Pb}$  dates and sedimentation rates of core ALB11B calculated using the CRS model. The CRS dating model places 1963 at a depth of c. 8.25 cm and is in good agreement with the  $^{137}\text{Cs}$  and  $^{241}\text{Am}$  records. Sedimentation rates in the core for the period from the 1860s to 1980s are relatively uniform with a mean value at  $0.031 \text{ g cm}^{-2} \text{ yr}^{-1}$ , apart from a small increase in the 1920s. However, sedimentation rates have increased in the last 20 years or so (Figure 12; Table 14).

**Table 12.  $^{210}\text{Pb}$  concentrations in core ALB11B taken from an Albertan lake, Canada.**

Depth cm	Dry Mass $\text{g cm}^{-2}$	Total		Pb-210 Supported		Unsupp		Cum Unsupported Pb-210	
		$\text{Bq Kg}^{-1}$	$\pm$	$\text{Bq Kg}^{-1}$	$\pm$	$\text{Bq Kg}^{-1}$	$\pm$	$\text{Bq m}^{-2}$	$\pm$
0.25	0.0446	396.39	45.5	20.27	12.35	376.12	47.15	167.1	17
2.25	0.4431	297.73	23.61	28.03	6.67	269.7	24.53	1442.4	132.8
4.25	0.8112	389.02	32.15	33.96	7.07	355.06	32.92	2584.8	176.2
6.25	1.2357	440.67	33.15	21.59	7.07	419.08	33.9	4224.5	237.3
8.25	1.6599	302.96	26.37	23.27	6.47	279.69	27.15	5686.6	284
10.25	2.0987	148.02	21.28	25.94	5.47	122.08	21.97	6520.8	308.7
12.25	2.6365	88.84	15.15	27.79	4.3	61.05	15.75	6994.4	327
14.25	3.1696	48.51	14.75	22.14	3.82	26.37	15.24	7214.7	337.7
16.25	3.7271	57.35	13.04	19.66	3.36	37.69	13.47	7391.4	347.5
18.25	4.2798	42.47	11.87	21.47	3.49	21	12.37	7549.1	355.2
20.25	4.8222	30.57	12.21	15.38	3.22	15.19	12.63	7646.4	361.6

**Table 13. Artificial fallout radionuclide concentrations in core ALB11B.**

Depth cm	Cs-137		Am-241	
	Bq kg <sup>-1</sup>	±	Bq kg <sup>-1</sup>	±
0.25	172.86	9.87	0	0
2.25	198.46	7.11	0	0
4.25	174.23	6.97	4.22	2.86
6.25	178.27	7.22	4.33	3.13
8.25	244.97	7.86	6.67	2.67
10.25	163.6	5.47	0	0
12.25	74.64	3.7	0	0
14.25	44.64	2.68	0	0
16.25	27.4	2.23	0	0
18.25	25.13	2.2	0	0
20.25	14.17	1.8	0	0

**Table 14. <sup>210</sup>Pb chronology of core ALB11B taken from an Albertan lake, Canada.**

Depth cm	Drymass g cm <sup>-2</sup>	Chronology			Sedimentation Rate		
		Date AD	Age yr	±	g cm <sup>-2</sup> yr <sup>-1</sup>	cm yr <sup>-1</sup>	± %
0	0	2006	0				
0.25	0.0446	2005	1	2	0.0628	0.319	13.3
2.25	0.4431	1999	7	2	0.0728	0.38	10.5
4.25	0.8112	1993	13	2	0.0453	0.229	10.9
6.25	1.2357	1981	25	2	0.0262	0.123	10.8
8.25	1.6599	1964	42	3	0.023	0.107	14
10.25	2.0987	1947	59	5	0.0314	0.128	22.8
12.25	2.6365	1931	75	6	0.0386	0.144	32.2
14.25	3.1696	1920	86	8	0.0633	0.232	61.7
16.25	3.7271	1907	99	9	0.0297	0.107	44.4
18.25	4.2798	1889	117	12	0.0299	0.109	67.2
20.25	4.8222	1868	138	16	0.0214	0.078	75.8

Figure 11. Fallout radionuclide concentrations in core ALB11B showing (a) total  $^{210}\text{Pb}$ , (b) unsupported  $^{210}\text{Pb}$ , and (c)  $^{137}\text{Cs}$  and  $^{241}\text{Am}$  (dotted line) concentrations versus depth.

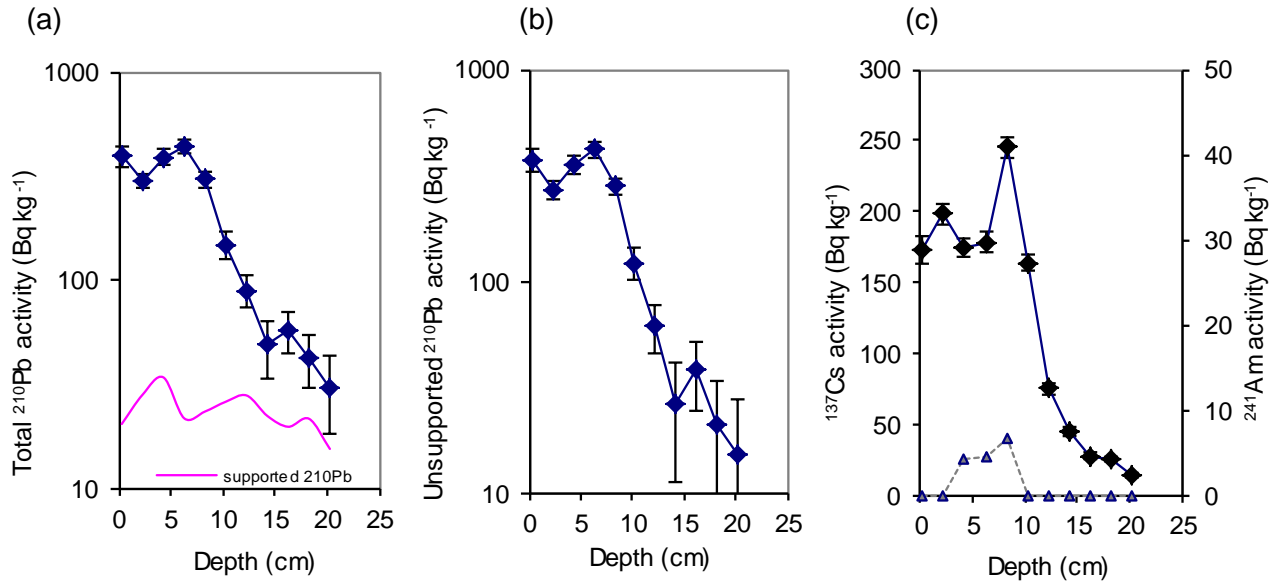
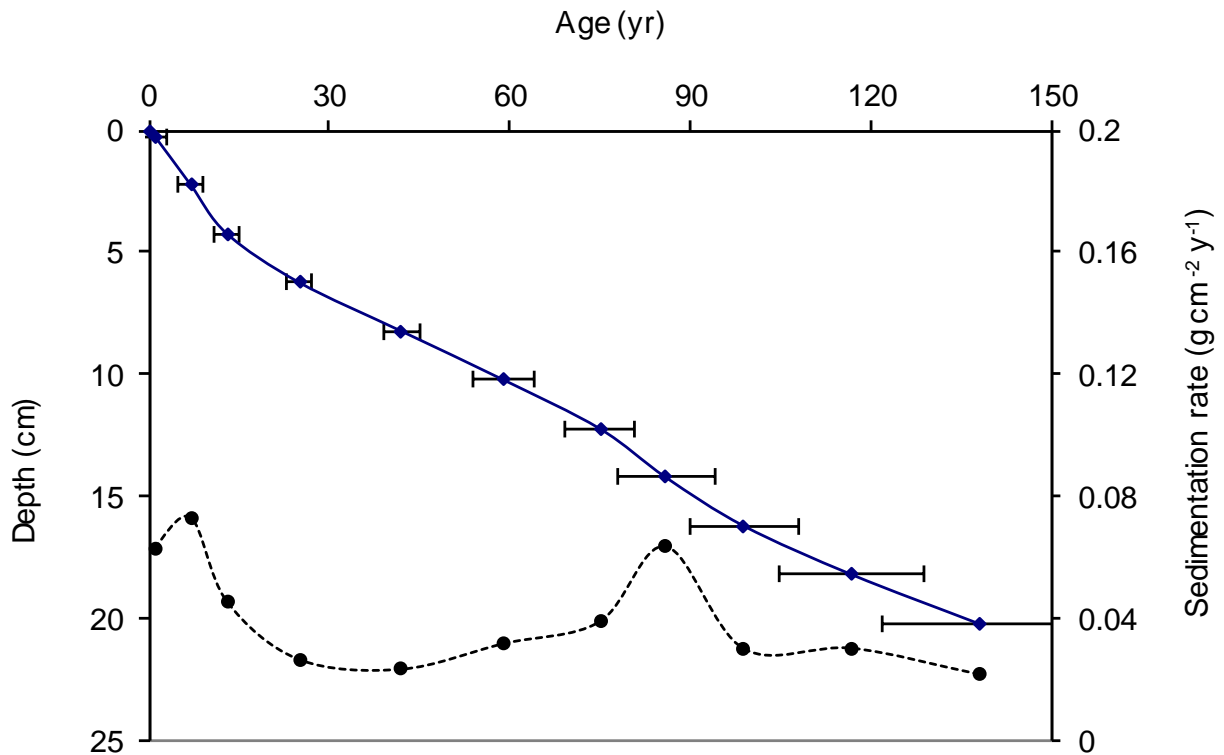


Figure 12. Radiometric chronology of core ALB11B showing the CRS model  $^{210}\text{Pb}$  dates and sedimentation rates. The solid line shows age while the dashed line indicates sedimentation rate.



### Trace element analyses

X-ray fluorescence spectroscopy analysis has been completed on the following cores ALB03B, ALB12B and ALB21B. Data for these cores are shown in Figure 13 – 15 respectively. Once all data are collated we will calculate enrichment factors for these elements and use a combination of these data with the outputs from the lithostratigraphic and sediment chronological work to determine dates at which significant changes in inputs and enrichments occurred as well as to calculate rates of change in inputs (fluxes) on a chronological basis.

**Figure 13. XRF analysis of cores ALB03B**

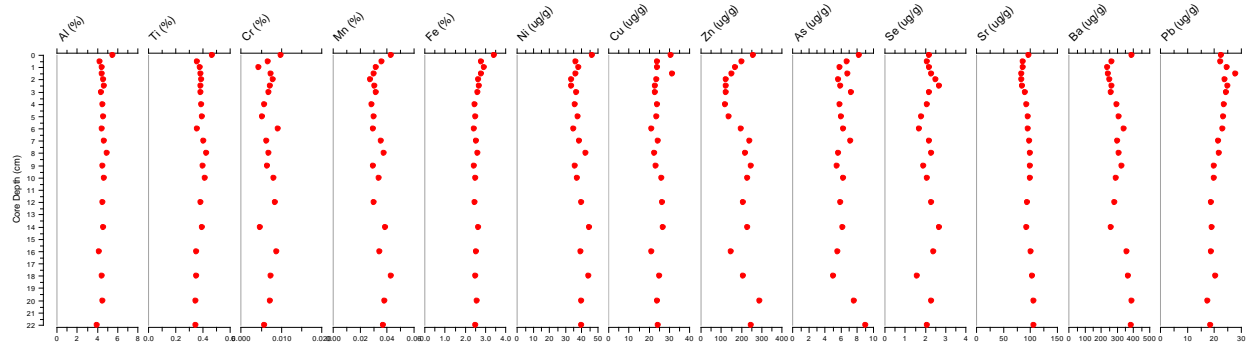


**Figure 14. XRF analysis of cores ALB12B**

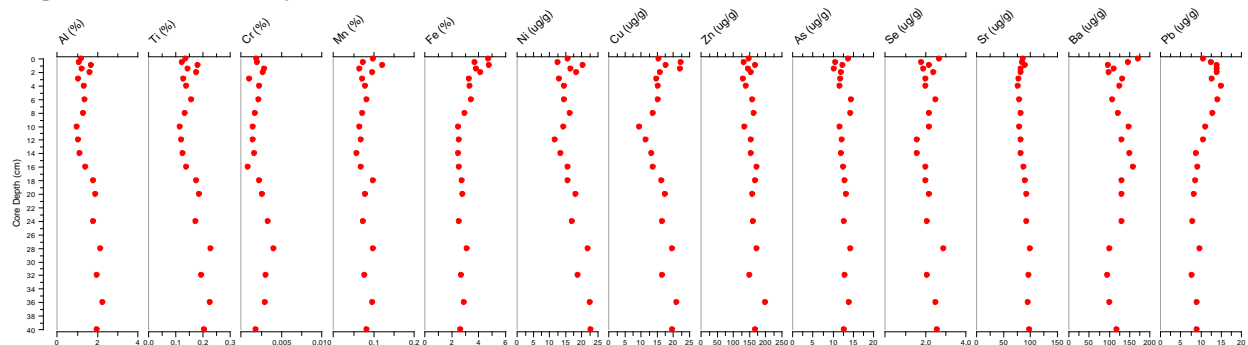
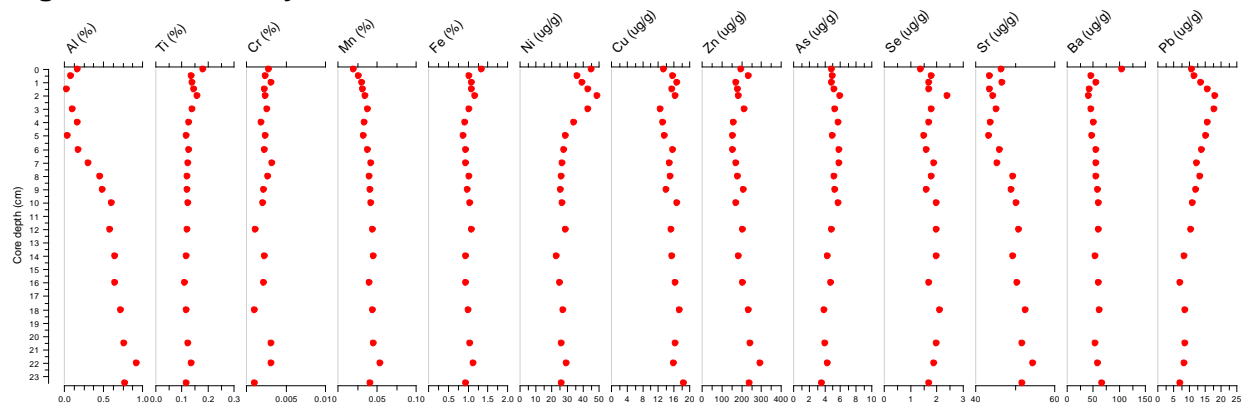


**Figure 15. XRF analysis of cores ALB21B.**

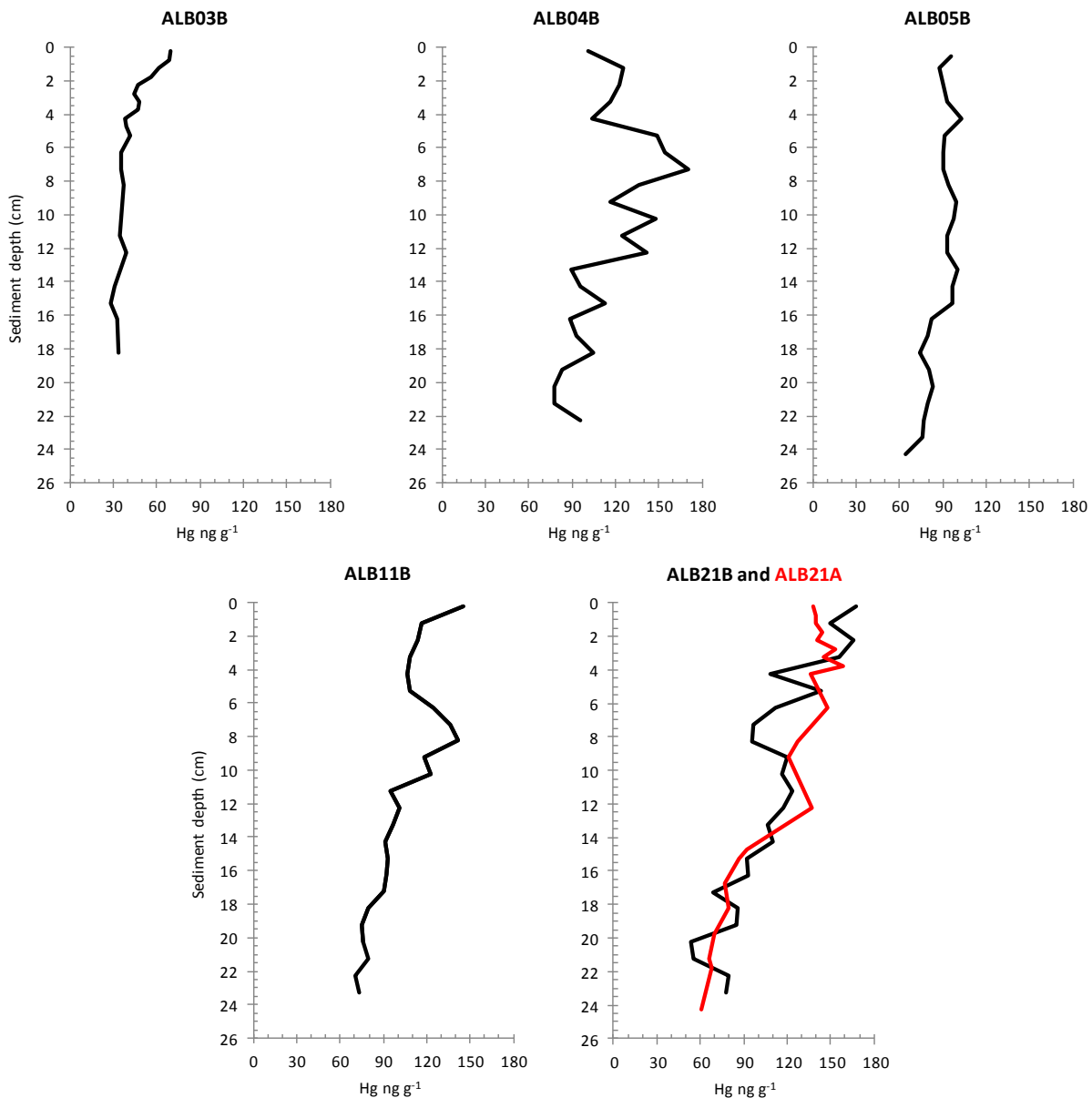


### Mercury data

Mercury analysis has been completed on ALB03B, ALB04B, ALB05B, ALB11B and ALB21B. Data for these cores are shown in Figure 16. As with the LOI data, the Hg profile and concentrations in ALB21B were consistent with the data from ALB21A analysed in the previous project and reported in Curtis et al (2010). These data are also presented in Figure 16 (red line) for comparison.

Once all data are collated we will calculate Hg enrichment factors and use a combination of these data with the outputs from the lithostratigraphic and sediment chronological work to determine dates at which significant changes in inputs and enrichments occurred as well as to calculate rates of change in inputs (fluxes) on a chronological basis.

**Figure 16. Mercury analysis of cores ALB03B, ALB04B, ALB05B, ALB11B and ALB21B. Profile for ALB21B also shows ALB21A from Curtis et al (2010) (red line) for comparison.**





## Work Outstanding

The following work remains to be completed

### Lithostratigraphy

- None. All work completed

### Core chronologies

- AL09B; ALB12B; ALB15B; ALB16B; ALB21B remain to be analysed

### Mercury analysis

- AL09B; ALB12B; ALB15B; ALB16B remain to be analysed

### Trace metal analysis

- ALB04B; ALB05B; ALB09B; ALB11B; ALB15B; ALB16B remain to be analysed

### Reporting and manuscript submission.

- A final report will be written on completion of this work and a manuscript prepared for submission to a peer-reviewed scientific journal.

## References

- Appleby, P G, 2001. Chronostratigraphic techniques in recent sediments. In W M Last and J P Smol (eds.) Tracking Environmental Change Using Lake Sediments. Vol. 1: Basin Analysis, Coring, and Chronological Techniques. Kluwer Academic Publishers, Dordrecht. Pp171-203.
- Appleby, P G, Richardson, N, Nolan, P J, 1992. Self-absorption corrections for well-type germanium detectors. *Nucl. Inst. & Methods B*, 71: 228-233.
- Appleby, P G, Nolan, P J, Gifford, D W, Godfrey, M J, Oldfield, F, Anderson, N J & Battarbee, R W, 1986. <sup>210</sup>Pb dating by low background gamma counting. *Hydrobiologia*, 141: 21-27.
- Curtis, C.J., Flower, R.J., Rose, N.L., Shilland, J., Simpson, G.L., Turner, S.D., Yang, H., Pla, S., 2010. Palaeolimnological assessment of lake acidification and environmental change in the Athabasca Oil sands Region, Alberta. *Journal of Limnology* 69 (Suppl.1), 92-104.
- Heiri, O., Lotter, A.F. and Lemcke, G. 2001. Loss on ignition as a method for estimating organic and carbonate content in sediments: reproducibility and comparability of results. *Journal of Paleolimnology* 25: 101–110, 2001.
- Kelly, E.N., Schindler, D.W., Hodson, P.V., Short, J.W., Radmanovich, R., Nielsen, C.C., 2010. Oil sands development contributes elements toxic at low concentrations to the Athabasca River and its tributaries. *Proceedings of the National Academy of Science* 107, 16178-16183.